

## Mechanical Properties and Metallurgical Characterization of LM25/ZrO<sub>2</sub> Composites Fabricated by Stir Casting Method

Karthikeyan Govindan <sup>1</sup>, Jinu GowthamiThankachi Raghuvaran <sup>2</sup>

<sup>1</sup> Department of Mechanical Engineering, University College of Engineering, Pattukkottai, Rajamdram, 614701, Thanjavur, Tamilnadu, India.

<sup>2</sup> Department of Mechanical Engineering, University College of Engineering Nagercoil, 629004, Konam, Tamilnadu India.

e-mail: p\_gkarthikeyan@yahoo.co.in, gr\_jinu1980@yahoo.com

### ABSTRACT

Zirconia (ZrO<sub>2</sub>) dispersed aluminum alloy metal matrix composites produced by stir casting techniques. Using stir casting techniques, aluminium based composites with varying amounts of 3%, 6%, 9%, and 12% of zirconia by weight are fabricated. The prepared samples were subjected to physical, mechanical, tribology and microstructure investigation. The extraordinary performance of Aluminium MMCs was the low density that obtained after alloying. Hardness and ductility were also increased when increase in Zirconia particle. Ultimate tensile strength, compressive strength and impact toughness were slightly increasing with the addition of zirconia particle. Microstructural characteristics shows that a homogeneous distribution of particles with reinforcement in casted composite. The investigations of the metallurgical characterization were carried using optical, scanning electron microscope, X-ray diffraction and Energy Dispersive Spectrometry (EDS) test to understand the metallurgical properties.

**Keywords:** Metal-matrix composites (MMCs), Hardness testing, Tensile test, Compression test, Scanning electron microscopy (SEM), Energy Dispersive Spectrometry (EDS).

### 1. INTRODUCTION

Novel innovations and surging needs in automobile industry ask for modified metal matrix composites [1, 2]. Metal Matrix Composites (MMCs) have emerged as an important class of materials for structural, wear, thermal, transportation and electrical applications because it offers high strength to weight ratio, high stiffness and good wear resistance [3-4]. The aluminum based metal matrix composites are excellent novel materials for applications in aerospace, automotive and transportation industries [5-6]. The fabrication methods of the aluminum based composites can be categorized into three processes: solid-state methods, semisolid state methods and liquid state method [5-6]. The stir casting is a liquid state method of composite fabrication, in which a dispersed phase is mixed with a molten matrix metal by means of mechanical stirring [7-8].

The addition of a ceramic reinforcement phase in monolithic metal alloys significantly alters their mechanical and physical properties, as well as their deformation behavior [9-12]. The Aluminum LM25 alloy is of low density and high thermal conductivity. However, the wear resistance is poor [13-15]. In order to avoid this drawback, this LM25 alloy reinforced with ZrO<sub>2</sub> to form LM25- ZrO<sub>2</sub> composites. This composite is used for marine casting, motorcar, engine parts, switch boxes, hydraulic systems (Piston, Cylinder) and food-processing industries. The ceramic materials are generally used to reinforcement aluminum alloys like SiC, TiC, TiB<sub>2</sub>, ZrB<sub>2</sub>, AlN, Si<sub>3</sub>N<sub>4</sub>, Al<sub>2</sub>O<sub>3</sub> and SiO<sub>2</sub> [3-4, 10, 12,14-15]. Among all the reinforcements used in aluminum based composites ZrO<sub>2</sub> particulates alone have shown their potential superiority in improving mechanical properties and microstructure further ZrO<sub>2</sub> particulates provides noticeable weight saving too [16-17]. In this field, Aluminium is the most popular matrix for the metal matrix composites. Most of the research works deal with aluminium matrix because of its natural light weight.

The Al alloys are quite attractive due to their low density, good corrosion resistance, processing flexibility, high thermal and electrical conductivity, improved elastic modulus, strength and their high damping capacity. Different processing techniques are used in the production of aluminium metal matrix

composites. They are squeezed casting infiltration, stir-casting, spontaneous infiltration, gas pressure infiltration, vacuum, centrifugal infiltration, hot pressing, cold pressing, powder extrusion, powder forging, diffusion bonding, etc. Among these methods Stir casting technique is used to produce the composites in economical way, high production rate at the very simple manner. It also increases the uniform distribution of particles and reduces the defects such as porosity, weak bonding between matrix and reinforcement [18-20].

The reinforcement of  $ZrO_2$  is very attractive as it exhibits a density of  $8.18 \text{ gm/cm}^3$ , melting point  $1860^\circ\text{C}$ , UTS-425 MPa, VHN-150, Young's modulus of 98 GPa. It was also found that  $ZrO_2$  shows better strength, hardness and fracture toughness with slight reduction in ductility [18, 20-21].

From the literature survey, it is identified that MMCs play a vital role in replacing metals, due to its advanced mechanical and metallurgical properties. A lot of researchers had concentrated in developing new composites such as Al 6061, LM25 and LM6 reinforcing with various elements such as  $TiB_2$ , SiC, TiC,  $ZrB_2$ , AlN,  $Si_3N_4$ ,  $Al_2O_3$  and their mechanical and metallurgical properties were analyzed in earlier researchers [5, 7-8, 11, 13-15, 20-21]. Very few works were identified in analyzing the effect of  $ZrO_2$  on mechanical and metallurgical properties. No works have been identified in analyzing the effect of  $ZrO_2$  on LM25 base material while subjected to mechanical and metallurgical properties. Hence the works mainly concentrated in developing new composite material by taking LM25 as the base material and varying percentage of  $ZrO_2$  to identify the influence of  $ZrO_2$  on the mechanical and metallurgical properties.

## 2. MATERIALS AND METHODS

### 2.1 Materials selection

In this work LM25 was selected as matrix materials for this investigation and it was reinforced with various weight percentages of  $ZrO_2$ , in order to overcome failure due to wear for the wide application in automobile and aircraft industries. The corresponding chemical compositions and mechanical properties of LM25 and  $ZrO_2$  are given in Tables 1 and 2 respectively.

**Table 1:** Chemical composition of LM25, LM6 Aluminium alloy and  $ZrO_2$  particles (wt %)

Chemical composition	Cu	Mg	Si	Fe	Mn	Ni	Zn	Pb	Sn	Ti	Al
LM25 alloy	0.1	0.2-0.6	6.5 – 7.5	0.5	0.3	0.1	<b>0.1</b>	<b>0</b>	<b>0.1</b>	<b>0.2</b>	<b>Bal</b>
Chemical composition of $ZrO_2$	$SiO_2$		$TiO_2$	$Fe_2O_3$			$Y_2O_3$		Zr		
	0.25%		0.16%	0.07%			3 to 5%		Bal		

### 2.2 Stir Casting Procedure:

The Aluminium LM25 alloy was taken as the base material and  $ZrO_2$  powder (Particle size 1-10 $\mu\text{m}$ ) was chosen as the reinforcement material. The corresponding chemical compositions are given table 1 & 2 respectively. In this work, six casted samples were prepared by keeping LM25 as the base material at varying weight percentage of  $ZrO_2$  such as 0%, 3%, 6%, 9%, 12% and 15%. The casting was carried out using stir casting process as shown in fig 1. Initially Aluminum LM25 alloy was melted in a pot by heating in a blower furnace at  $850^\circ\text{C}$  for 15 min. The  $ZrO_2$  powder was preheated at  $575^\circ\text{C}$  in a separate muffle furnace. The furnace temperature was raised above liquid temperature of LM25 at about  $850^\circ\text{C}$  to melt the LM25 completely and then it is added to the preheated  $ZrO_2$  powder slowly. The stirring was carried out with help of the drilling machine for about 15 minutes and the stirring rate maintained the speed of about 950 rpm. This combination was then transferred into mould cavity, and it is cooled in a room temperature. This procedure was followed for the preparation of six specimens with different compositions of  $ZrO_2$  as shown in fig 1.



1. Preheating Furnace
2. Control Unit
3. Main Furnace
4. Stirrer

**Figure 1:** Stir Casting Machine

### 2.3 Density Measurements Test

The density of a material plays a vital role in Al MMCs. It was estimated by theoretically and experimentally in order to find its accurate density value. Rule of mixture is a method of approach to find out theoretical estimation of composite material, based on the assumption that a composite property is the volume weighted average of the matrix and reinforcement phase properties. Then, the density of fabricated Aluminium LM25/ZrO<sub>2</sub> metal matrix composite was measured by Archimede's principle for experimental calculation. The density measurement involved weighing the polished sample specimen in air and when immersed in distilled water.

### 2.4 Hardness test

Micro hardness test was conducted on the polished samples of aluminium LM 25 alloy and its composites by adopting standard testing procedure. The hardness of the composite was measured using Vickers micro hardness tester as per ASTM: E384-10. All the samples were applied with a load of 300 g for a period of 10 s. The test was carried out at three different locations to avoid the possible effect of the indenter resting on the hard reinforcement particles. The averages of all the six readings were reported.

### 2.5 Tensile Test

The eighteen tensile test sample specimens were prepared as per the ASTM standard (ASTM B-557-M-94), and it was tested in a Universal Testing Machine (FIE Pvt.Ltd., model: unitek 94100) . Before measuring the tensile strength, the eighteen samples were machined into cylindrical shape. Three samples were tested for each composition to obtain the best tensile test result.

### 2.6 Compression test

The compression test sample specimens were prepared as per the ASTM standard (ASTM D695), and it was tested in a Universal Testing Machine (FIE Pvt.Ltd., model: unitek 94100). In general, an aluminium alloy shows an apparently higher strength in compression than in tension. Compression tests are of extremely high commercial importance, because it helps to determine material properties. The compression tests were carried out according to ASTM standard. The tests were conducted on a universal testing machine. For this test, three different sample specimens were prepared for the different volume fractions of ZrO<sub>2</sub> particles with Aluminium LM25 based MMCs

### 2.7 Impact Test

The eighteen impact test sample specimens were prepared as per the ASTM standard (ASTM A370), According to this standard, the standard specimen size for Charpy impact testing is 10 mm × 10mm × 55mm. The impact test of the material can be obtained by Charpy or Izod test. Impact properties are not directly used for fracture calculations but economically impact tests can be used as a quality control method to notch sensitivity. It is further used to compare the relative toughness of engineering materials.

## 2.8 Microstructure Analysis

Microstructure Analysis is usually conducted to determine the material's response to thermal heat treatment. Every metal and nonmetal have a preferred microstructure created or modified by processing and heat treatment. The Microstructure is the "fingerprint" of material processing. The Microstructure of a composites is analyzed to know the difference between the Matrix metal and the composite after stir casting. The microstructure is revealed by selective etching with the H.F acid solution and observed using an optical microscope. In case of composites, the microstructure is also done to see the distribution of reinforcement particles and reinforcement matrix interfacial bonding. The samples have been prepared, and the preparation for examination was done by grinding through 320, 400, 600, 800, 1200 and 1500 grit papers followed by polishing with alumina paste. Then the samples were etched with Keller's reagent to obtain a better contrast. The etched samples were dried, and the microstructure was observed by using the scanning electron microscope at different magnification. For this study, optical and scanning electron microscopes were used for microstructure analysis.

## 3. RESULTS AND DISCUSSION

The results obtained from the various mechanical, metallurgical tests for the cast are as discussed in detail below.

### 3.1 Mechanical test results for LM25-ZrO<sub>2</sub> composites

This section mainly illustrates and discusses in details about the various results obtained from mechanical testing of the developed composites

#### 3.1.1 Effect of Density

The experimentally evaluated densities are derived from the recorded weights and then compared to the theoretical rule of mixture of densities, which is almost relevant to experimental values. The comparisons of densities by rule of mixture and Archimede's principle are shown in Figure 2. From the table, it is clearly identified that the density was gradually increased by the addition of ZrO<sub>2</sub> particle with aluminium LM25 alloy. Therefore, this clearly reveals that the densities is increases with increasing percentage of ZrO<sub>2</sub> as shown in Figure 2. Similar trends have been observed by many other researchers [8, 21].

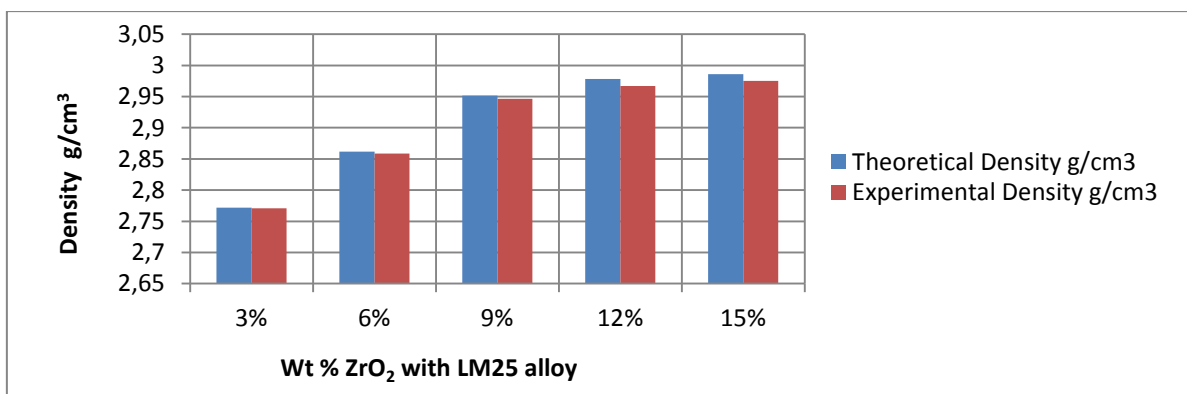


Figure 2: Comparisons of Theoretical and Experimental density

#### 3.1.2 Effect of Tensile strength

The tensile test results indicating yield, ultimate tensile strength and percentage of elongation of the six specimens LM25 reinforced with 0%, 3%, 6%, 9%, and 12% respectively are given in the fig 3. From the fig, it is clearly identified that the maximum ultimate tensile strength is obtained for the sample 5 that contains 12 % of ZrO<sub>2</sub>. Therefore, this clearly reveals that the ultimate tensile strength is increases with increasing percentage of ZrO<sub>2</sub> as shown in figure 3. Similar trends have been observed by many other researchers. Similar trends have been observed by many other researchers [8, 18].

### 3.1.3 Effect of Compression Strength

The results are shown in Fig 4. From this, it was observed that with the increase in the volume fraction of  $ZrO_2$  particle, increases the compressive strength. The increased volume fraction of  $ZrO_2$  particle mixture gives maximum compressive force that could be withstood by the material.

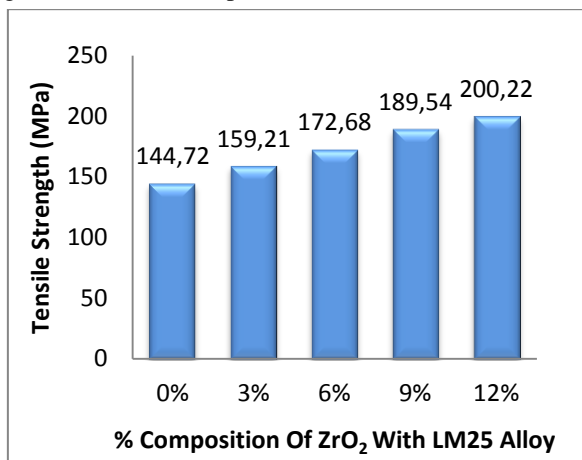


Figure 3: Effect of Tensile strength

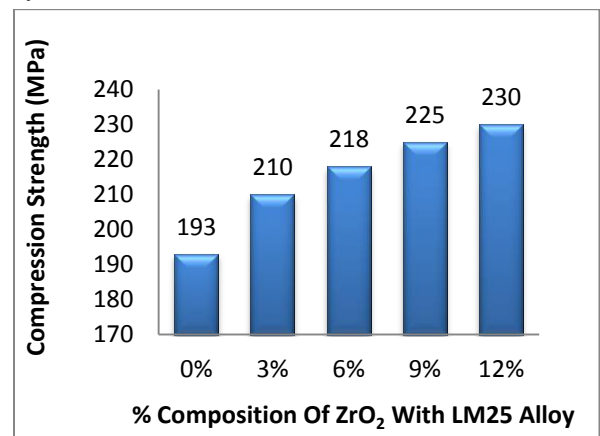


Figure 4: Effect of compressive Strength

### 3.1.4 Effect of Impact strength

The results of the Charpy impact tests for Aluminium LM25 composites fabricated with the different volume fractions of  $ZrO_2$  particle are shown in Fig 5. The test results reveals that the impact energy of Aluminium LM25/ $ZrO_2$  based metal matrix composite mainly depends on the distribution of the particles in the matrix. It was interesting to note that there was no variation in the value of the Base Metal and 3% Volume fraction of  $ZrO_2$  particles with Aluminium LM25 were shown in Fig 5. The impact values were slightly increased with increasing volume fraction of  $ZrO_2$  of particle after 3% of  $ZrO_2$ .

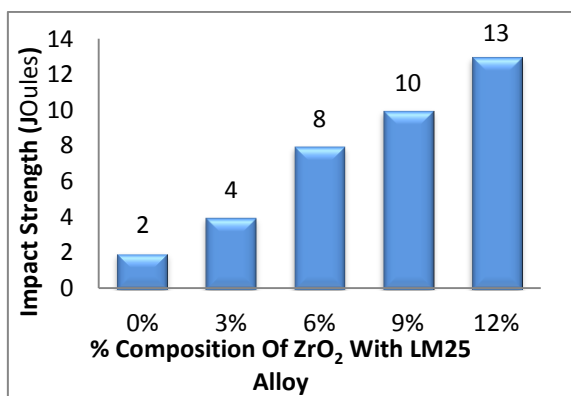


Figure 5: Impact strength of LM25 with various Wt %  $ZrO_2$

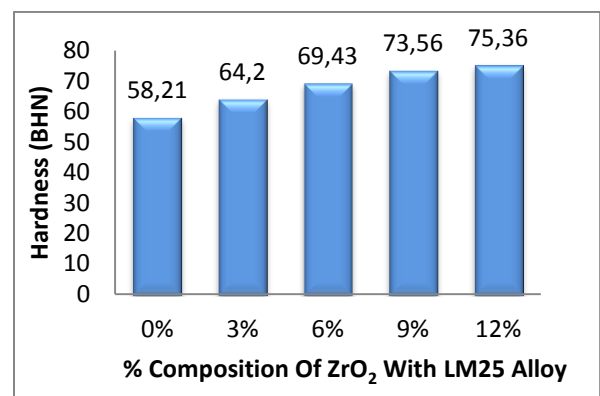


Figure 6: Hardness value with varying wt% of  $ZrO_2$

### 3.1.5 Effect of hardness

The hardness of the composite depends upon the reinforcement of matrix material. As the coefficient of thermal expansion of Zirconia is less than the aluminium alloy, an enormous amount of dislocations is generated at the particle-matrix interface during a solidification process. This makes the further increases in the hardness of the matrix [8]. The hardness test was conducted on Brinell hardness equipment for a load of 500 kg. The results are graphically shown Fig.6. It is observed that the hardness values of the material is directly proportional to the presence of  $ZrO_2$  with the increase in  $ZrO_2$ , the hardness increases. Similar trends have been observed by many other researchers [5, 20].

### 3.1.5 Effect of Ductility

Figure 7 is a graph showing the effect of  $ZrO_2$  content on the ductility of cast LM25/  $ZrO_2$  particulate composites. From the fig 7, it can be seen that,  $ZrO_2$  content increases, the ductility of the composite material increases monotonically by significant amounts. Therefore it clearly reveals that, the maximum ultimate ductility is obtained for the sample 5 that contains 12 % of  $ZrO_2$ .

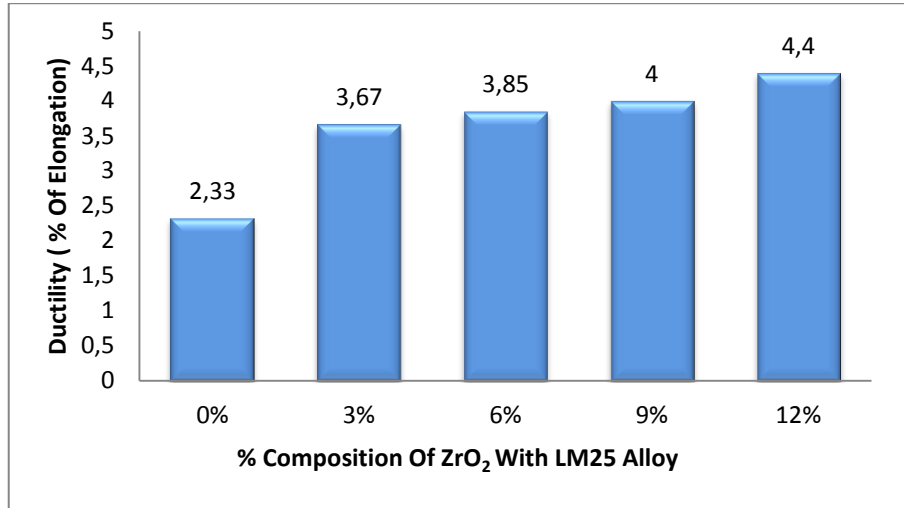


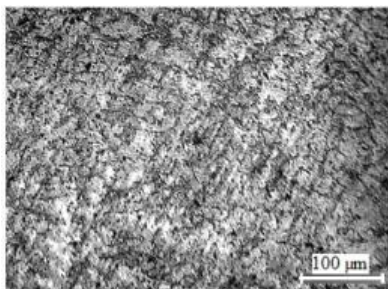
Figure 7: Variation in Ductility with wt% of  $ZrO_2$  for LM25/ $ZrO_2$  Composites

### 3.2 Metallurgical Characterization

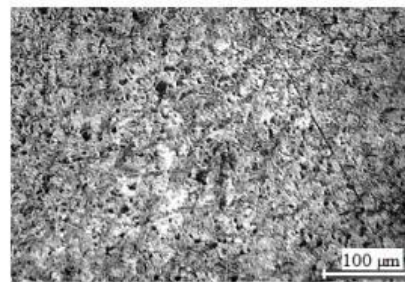
This section mainly illustrates and discusses in details about the various results obtained from metallurgical testing of the Cast LM25- $ZrO_2$  composite specimens

#### 3.2.1 Analysis of optical microscopy:

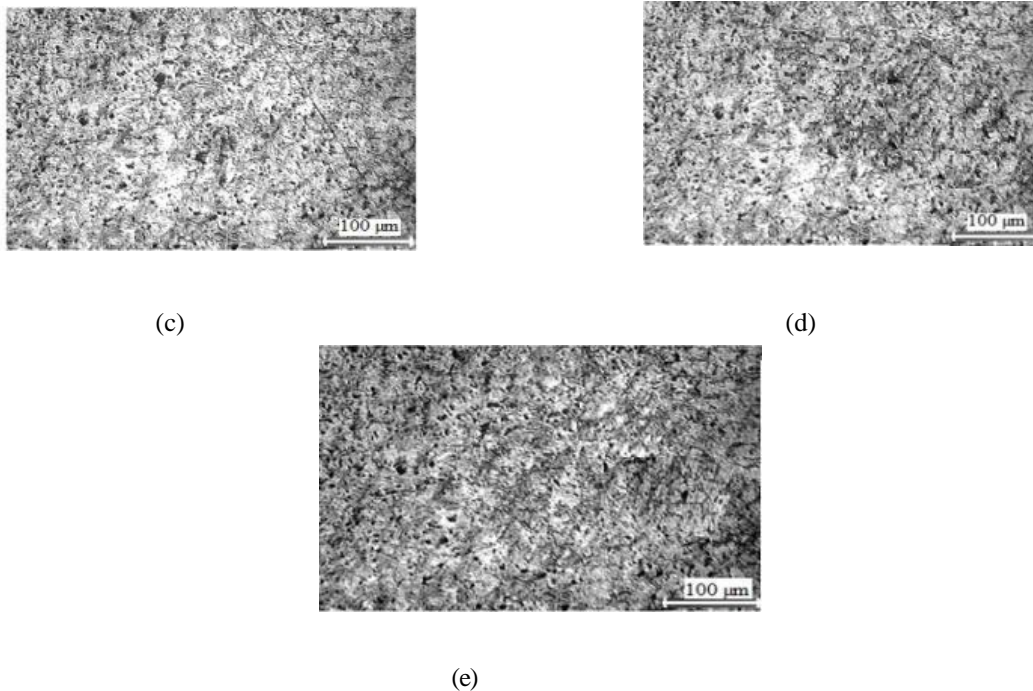
In this work,  $ZrO_2$  is added as reinforcement for aluminium alloy LM25 series to analyze the change in the properties of the matrix metal. As a part of it, the wider effort is taken to improve the performance of LM25/ $ZrO_2$  composites. This research sets out to investigate the effect of minor elements (Zirconia) on castability. This is clear from the Figure 8 (a-e), which shows optical microscopy images. The LM25/ $ZrO_2$  composites show fine grains of Al-Zr eutectic in aluminium solid solution. The constituents of phases present in the matrix are  $Mg_2Si$  and some Cu- $Al_2$  phases which are randomly distributed. The Al-Si eutectic forms an interdendritic pattern due to rapid cooling. As it is chilled, the cast shows that the dendritic pattern of the grains is cured towards the direction of the chilled plate. No directional orientation could be seen in castings. The presence of  $ZrO_2$  in the aluminium matrix alloy is uniform and present as dark particles.



(a)



(b)

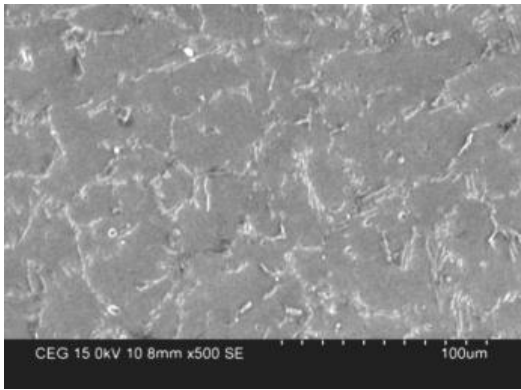


**Figures 8:** Optical Microscopic image of various composite specimens a) LM25 alloy (b) LM25–3% of ZrO<sub>2</sub> (c) LM25–6% of ZrO<sub>2</sub> (d) LM25–9% of ZrO<sub>2</sub> (e) LM25–12% of ZrO<sub>2</sub>

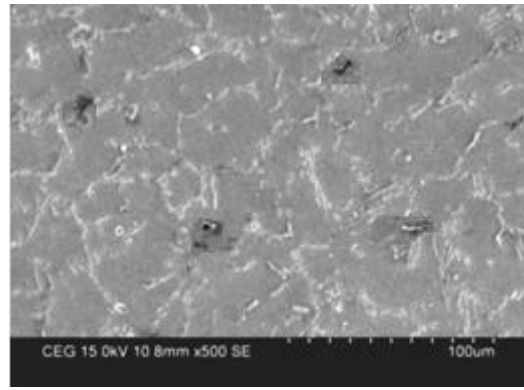
### 3.2.2 Analysis of scanning electron microscopy images

On viewing Figures 9 (a-e), it was found that the particle size of the Zirconia is very fine. This is why, at 100μm, the particles look very small, and it can be easily detected that the distribution of the particles is almost uniform. Scanning Electron Microscope test micrographs (SEM) images of the different weight fraction of ZrO<sub>2</sub> particles with LM25 are shown in Figure 9 (a-e). From these SEM images, it is clearly identified that the distribution of particles throughout the matrix was found to be fairly uniform as a dark region. Scanning Electron micrographs at lower magnification shows the distribution of ZrO<sub>2</sub> particles throughout the aluminium MMCs and at higher magnifications, the Scanning Electron Microscopes results show the particle-matrix interfaces. From these figures, it is clearly revealed the homogeneous distributions of ZrO<sub>2</sub> reinforced particles with aluminium alloy occurred. Further, these figures reveal the homogeneity of the cast composites. The properties of the aluminium MMCs depend not only on the matrix particle and the weight fraction but also on the distribution of reinforcing particles and interface bonding between the particle and matrix.

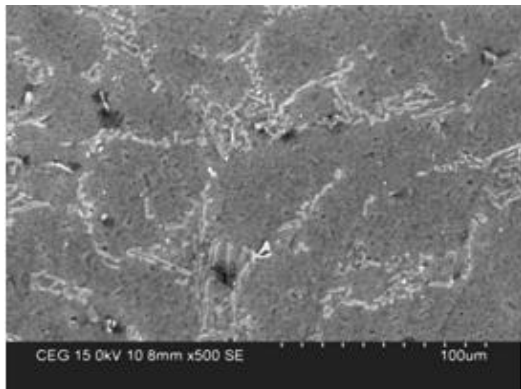
The relationship between the distribution of particles and weight fraction of Zirconia is studied from Scanning Electron Micrographs. In either case, no pores have been observed, which indicates better wettability between the matrix and reinforcement particles. So the interfacial bonding was obtained in the case due to rapid cooling. It is also observed that as the weight percentage of reinforcement of ZrO<sub>2</sub> increases, the area fraction also increases as shown in the micrographs as a dark region. It can also be noticed that the average grain size of Aluminium LM25 matrix decreases with increase in the weight fraction of ZrO<sub>2</sub> reinforcement. It is also inferred that there is an increase in mechanical properties due to the increase in the interfacial bonding of reinforcement with the aluminium matrix alloy. This is due to the gravity of ZrO<sub>2</sub> and it is associated with judicious selection of stirring parameters and good wetting of preheated ZrO<sub>2</sub> particulates before adding in the matrix alloy.



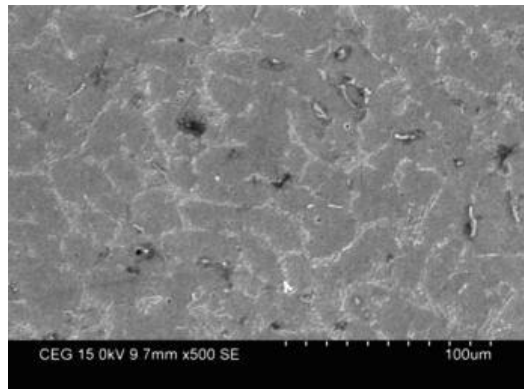
(a)



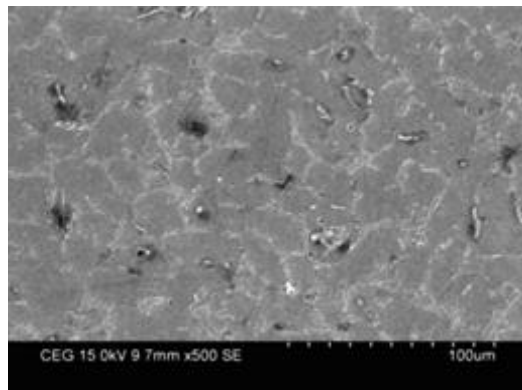
(b)



(c)



(d)



(e)

**Figures 9 (a-e):** SEM images of various composite specimens (a) LM25 alloy (b) LM25–3% of ZrO<sub>2</sub> (c) LM25–6% of ZrO<sub>2</sub> (d) LM25–9% of ZrO<sub>2</sub> (e) LM25–12% of ZrO<sub>2</sub>

**3.2.3 SEM-EDS Analysis with Element Distribution.**

The developed composite material was examined under Scanning Electron Microscope to find the formation of ZrO<sub>2</sub> particles and their surface morphology. X-diffraction test was carried out to confirm the formation of ZrO<sub>2</sub> phase's using D/MAX ULTIMA III XRD machine supplied by Rigaku Corporation (Rigaku-mini flex 600). X-ray diffraction pattern was obtained for the specimen using Cu k $\alpha$  radiation. The data were collected over the 2  $\theta$  for the range of 10° to 120° degree with a step size of 0.02° degree and the scan speed of 10 degree/min.

The X-ray diffraction pattern is well matched with the standard JCPDS (01-1176) of aluminium with a cubic crystal structure and Fm-3m space group. The absence of any additional peak other than aluminium in all the samples, confirms that the phase is the pure formation and no chemical reactions happen during casting process as shown in Figure 10.

However, a shift in all peaks (Table 4) upon ZrO<sub>2</sub> without any additional peak for ZrO<sub>2</sub>, confirms the addition of trace amount of ZrO<sub>2</sub>, well mixed with the parent aluminium without disturbing the parent phase. The change in lattice parameters, Crystalline Size and Cell Volume upon addition of ZrO<sub>2</sub> are shown in Table 5, which again confirms the above observation. A gradual marginal shift in the Al peaks to higher angles with an increase in the weight fraction of reinforcement is evident, which indicates a decrease in the lattice parameter of aluminium.

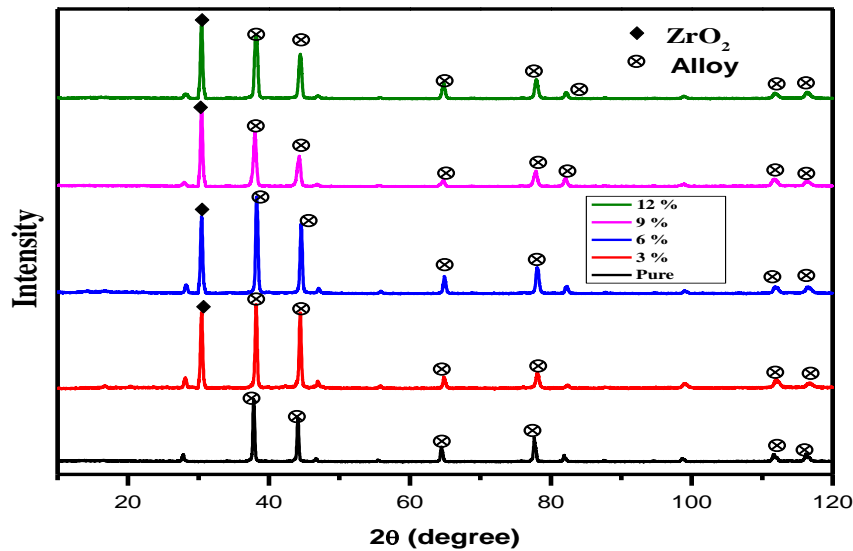


**Figure 10:** X-ray diffraction patterns of the specimen for LM25 with various wt% reinforcement of ZrO<sub>2</sub> Table 4 Peak position of LM25/ZrO<sub>2</sub> composites.

**Table 2:** Peak position of LM25/ZrO<sub>2</sub> composites

Peak No.	Peak Position 2 $\theta$ (Deg)				
	Pure	3%	6%	9%	12%
1	37.794	38.166	38.212	38.001	38.146
2	44.064	44.386	44.45	44.274	44.402
3	64.451	64.79	64.877	64.77	64.749
4	77.644	78.03	78.012	77.796	77.85
5	81.886	82.26	82.064	82.08	82.15
6	98.62	98.87	98.95	98.84	98.72
7	111.666	111.92	111.752	111.63	111.75
8	116.235	116.56	116.43	116.26	116.27

**Table 3:** Changes in Structural Parameters on addition of ZrO<sub>2</sub> on LM25 alloy JCPDS Al (01-1176)

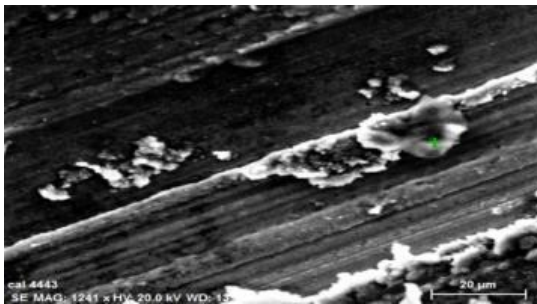
Sample	Lattice Parameter - a (Å)	Crystalline Size (Å)	Cell Volume (10 <sup>6</sup> pm <sup>3</sup> )
Pure	4.0644	6.41	67.14
3%	4.0545	4.08	66.65
6%	4.0564	4.28	66.75
9%	4.0605	3.16	66.95
12%	4.0594	3.60	66.90

### 3.2.3.1 Interpretation of XRD analysis:

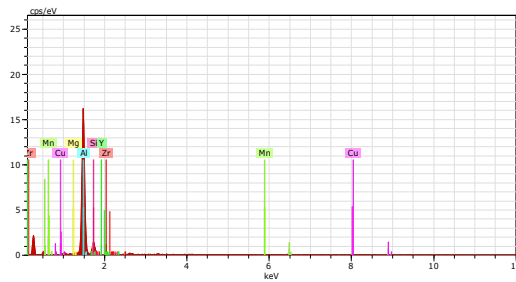
- The crystalline structure of Al and XRD diffraction phases is confirmed on comparison with JCPDS (01-1176).
- Diffraction peaks are present only for Al and no other impurities are present.
- ZrO<sub>2</sub> diffraction peaks are not present because precursor may not be dissolved in a solvent.

### 3.2.3 SEM-EDS Analysis with Element Distribution.

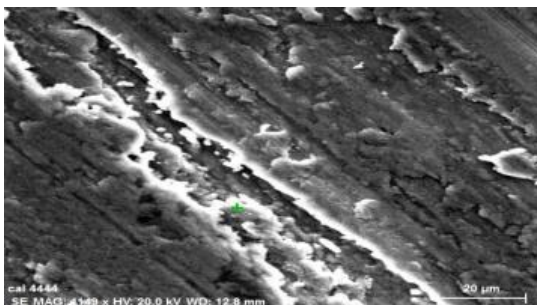
The Energy Dispersive Spectrometry (EDS) analysis had been applied to all prepared samples of various percentages of ZrO<sub>2</sub> before they were subjected to the wear test. The present section helps to find out information about the type of the element present in all the cast samples. Figure 11 (b), (d), (f) and (h) shows the EDS of aluminium LM25 with its elements. The Figure 11 (a), (c), (e) and (g) represents the topographical images taken using a Scanning Electron Microscope (SEM).



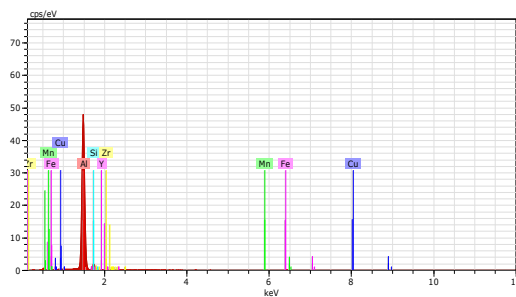
(a)



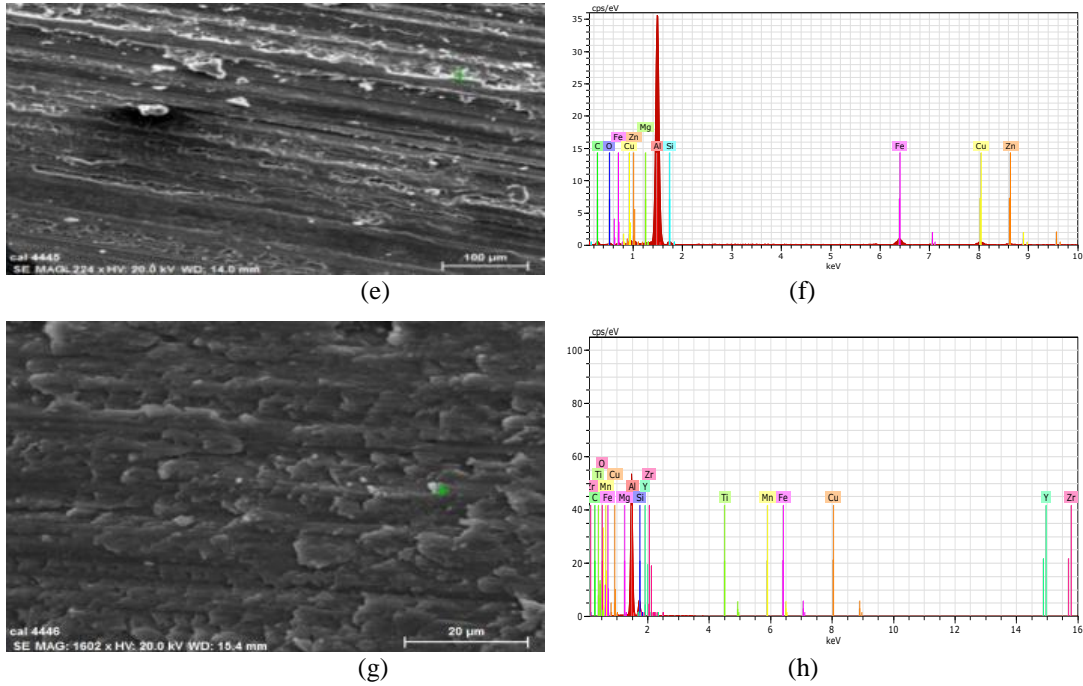
(b)



(c)



(d)



**Figures 11(a-h):** SEM images and EDS patterns of various composites (a) SEM image of LM25 (b) EDS pattern of LM25 (c) SEM image of LM25-3% ZrO<sub>2</sub> composites (d) EDS pattern of LM25-3% ZrO<sub>2</sub> composites (e) SEM image of LM25-6% ZrO<sub>2</sub> composites (f) EDS pattern of LM25-6% ZrO<sub>2</sub> composites (g) SEM image of LM25-9% ZrO<sub>2</sub> composites (h) EDS pattern of LM25-9% ZrO<sub>2</sub> composites.

The graphs obtained using EDS test show that, these results are used to confirm the chemical composition of the LM 25/ZrO<sub>2</sub> composites, such as aluminium, zirconium, iron, copper, magnesium, zinc, silicon and all other elements present in the prepared composites as shown in Figure 11 (b), (d) (f) and (h). The shrinkage and porosity were not identified in the micrographs. This is evidence of good quality castings. An increase in the percentage of ZrO<sub>2</sub> resulted in the oxide formation at the pin surface and the developed oxide's act as a wear protective layer for various loads. This is clearly seen in Figure 11 (d), (f) and (h). Finally, the EDS analysis confirmed the presence of aluminium and ZrO<sub>2</sub> particles, as shown in Figure 11 (d), (f) and (h).

#### 4. CONCLUSIONS

The Development of aluminium LM25/ZrO<sub>2</sub> composites for different weight proportions are experimentally studied. Then the following conclusions are made from experimental results.

This investigation analyzed the effect of various weight percentages of ZrO<sub>2</sub> with LM25 alloy on the mechanical properties and metallurgical characterization and the results obtained from these studies are summarized as follows:

- Physical test results of the developed LM25/ZrO<sub>2</sub> and composites revealed that the sample cast at 12 wt% of ZrO<sub>2</sub> reinforcement particles has a lower weight and all the cast samples are free from porosity.
- From the tensile test results, it is identified that the maximum tensile strength is found to be about 210 Mpa for 12 wt% reinforcement of ZrO<sub>2</sub> on LM25 alloy. Then the tensile tested samples are subjected to fractography investigation. The fractography results show that the increase in weight percentage of ZrO<sub>2</sub> changes the mode of failure from ductile to brittle nature, which is revealed from the occurrence of large dimple tiny particles with a large amount of plastic deformation present in the low weight percentages of ZrO<sub>2</sub> reinforced composites
- The compression test results reveal that the maximum compressive strength is about 230 Mpa for the sample containing 12 wt% of ZrO<sub>2</sub>.
- From the impact test results, it is identified that the best impact strength is about 15 joules and it is obtained from the sample containing 12wt % of ZrO<sub>2</sub>.
- The hardness test results reveal that the maximum hardness is about 78.5 BHN for the sample

containing 12 wt % of ZrO<sub>2</sub>.

- The microstructure results show that for higher weight percentage (12%) reinforcement of ZrO<sub>2</sub> shows a good uniform distribution, interfacial bonding and non-occurrence of porosity.
- The SEM images of various weight percentages of ZrO<sub>2</sub> reinforcement reveal that the SEM image for 12 wt % ZrO<sub>2</sub> contains more of the presence of ZrO<sub>2</sub> particles, which is clearly seen as a dark region.
- The EDAX results of the developed composites show that the presence of 12 wt% of ZrO<sub>2</sub> particle in LM25/ZrO<sub>2</sub> composites is higher which shows that the developed oxide layer acts as a wear protective layer.
- The XRD result shows that no phase transformation occurred in the developed composites, which clearly indicates that no chemical reactions are carried out during the casting process.

## 5. ACKNOWLEDGEMENTS

The authors acknowledge the support from Regional Centre, Anna University: Tirunelveli Region and University college of Engineering Nagercoil, India, to complete the work.

## 6. BIBLIOGRAPHY

- [1] SOZHAMANNAN, G.G., BALASIVANANDHA PRABU, S., VENKATAGALAPATHY, V. S. K., "Effect of Processing Parameters on Metal Matrix Composites: Stir Casting Process", *Journal of Surface Engineered Materials and Advanced Technology*, v.2, pp. 11-15, 2012.
- [2] UMIT CO CEN, KAZIM O' NEL, "Ductility and strength of extruded SiCp/aluminium-alloy composites", *Composites Science and Technology*, v.62, pp. 275–282, 2002.
- [3] LAKSHMI, S., LU, L., GUPTA, M., "In situ preparation of TiB<sub>2</sub> reinforced Al based composites, *J Mater Process Technology*, v.73, 160–166, 1998.
- [4] TAHAMTAN, S., HAVAEE, A., EMAMY, M., ZABIHI, M.S., "Fabrication of Al/A<sub>2</sub>O<sub>3</sub>-Al<sub>2</sub>O<sub>3</sub> Nano/micro composite by combining ball milling and stir casting technology", *Materials and Design*, v. 49, pp.347-359, 2013.
- [5] KARTHIKEYAN, G., JINU, G. R., "Dry Sliding Wear Behavior Optimization of Stir cast LM6/ZrO<sub>2</sub> Composites by Response Surface Methodology analysis", *Transactions of the Canadian Society for Mechanical Engineering*, v. 40, n. 3, pp.351-369, 2016.
- [6] TJONG, SC, TAM, KF, "Mechanical and thermal expansion behavior of hipped aluminum–TiB<sub>2</sub> composites", *Mater Chem Phys.*, v.97, pp. 91–97, 2006.
- [7] EZATPOUR, H.R., SAJJADI, S.A., SABZEVAR, M.H., *et al.*, "Investigation of microstructure and mechanical properties of Al6061-nanocomposite fabricated by stir casting", *Materials and Design.*, V.55, pp.921-928, 2014.
- [8] KARTHIKEYAN, G., JINU, G. R., " Experimental Investigation of Mechanical and Wear behaviour of Aluminium LM6/ZrO<sub>2</sub> Composite fabricated by stir casting method", *Journal of the Balkan Tribological Association*, v 21, n.3, pp.539-556, 2015.
- [9] YILMAZ, O., BUYTOZ, S., "Abrasive wear of Al<sub>2</sub>O<sub>3</sub>-reinforced aluminium-based MMCs", *Composites Science and Technology*, V.61, pp.2381–2392, 2001.
- [10] KARTHIKEYAN, R., RAGHUKANDAN, K., NAAGARAZAN, R.S., *et al.*, "Optimizing the Milling Characteristics of Al-SiC Particulate Composites", *Metals and Materials.*, v.6 , pp.539-547, 2000.
- [11] PERNG-CHENG CHEN., SU-JIEN LIN., "A Study on the Low-Cycle Fatigue Properties Of SiC<sub>p</sub>/6061 Al Composites", *Journal Of Materials Science.*, v.32, pp. 4153-4158, 1997.
- [12] VINOD KUMAR, G.S., MURTY, B.S., CHAKRABORTY, M., "Grain refinement response of LM25 alloy towards Al–Ti–C and Al–Ti–B grain refiners", *Journal of Alloys and Compounds.*, v.472, pp.112–120. 2009.
- [13] KADIR KOCATEPE, "Effect of low frequency vibration on porosity of LM25 and LM6 alloys", *Materials and Design.*, v. 28, pp.1767-1775, 2007.
- [14] ELANGO, G., RAGHUNATH, B.K., "Tribological behavior of hybrid (LM25Al+SiC+TiO<sub>2</sub>) metal matrix composites", *Procedia Engg.*, v.64, pp.671-680, 2013.

- [15] PRASADA RAO, A.K., DAS, K., MURTY, B.S., CHAKRABORTY, M., “Microstructural and wear behavior of hypoeutectic Al-Si alloy (LM25) grain refined and modified with Al-Ti-C-Sr master alloy”, *Wear.*, v.261, pp.133-139, 2006.
- [16] HEMANTH, J. “Development and property evaluation of aluminum alloy reinforced with nano- ZrO<sub>2</sub> metal matrix Composites”, *Material Science and Engineering A.*, v.507, pp.110-113, 2009.
- [17] JOEL HEMANTH, “Fracture behavior of cryogenically solidified aluminum-alloy reinforced with nano-ZrO<sub>2</sub> metal matrix composites”, *Journal of Chemical Engineering and Materials Science.*, v.2, n.8, pp.110-121, 2011.
- [18] KARTHIKEYAN, G., JINU, G, R., “Tensile Behaviour and Fractography Analysis LM6/ZrO<sub>2</sub> Composites”, *Materiali in Tehnologije / Materials and technology*, v. 51, n.3, pp.549-553, 2017.
- [19] DAS, S., BEHERA, R., DATTA, A., MAJUMDAR, G., *et al.*, “Experimental Investigation on the Effect of Reinforcement Particles on the Forgeability and the Mechanical Properties of Aluminium Metal Matrix Composites”, *Materials Sciences and Applications*, v. 1, pp.310-316, 2010.
- [20] KARTHIKEYAN, G., JINU, G.R., “Dry sliding wear behaviour of stir cast LM 25/ZrO<sub>2</sub> Metal Matrix Composites”, *Transactions of Famena*, v.39, n. 4, pp. 89-98, 2015.
- [21] KARTHIKEYAN, G., JINU, G, R., VIJAYALAKSHMI, P, “Weldability Study of LM25-ZrO<sub>2</sub> Composites by Using Friction Welding”, *Matéria (Rio de Janeiro)*, v. 22, n. 3, pp.1-12, 2017.

#### ORCID

Karthikeyan Govindan <https://orcid.org/0000-0002-0593-9960>  
Jinu Gowthami Thankachi Raghuvaran <https://orcid.org/0000-0002-1959-3630>